Optimizing an estuarine water quality monitoring program through an entropy-based hierarchical spatiotemporal Bayesian framework

Ibrahim Alameddine,[1,2] Subhankar Karmakar,[3] Song S. Qian,[1,4] Hans W. Paerl,[5] and Kenneth H. Reckhow[1]

[1] The total maximum daily load program aims to monitor more than 40,000 standard violations in around 20,000 impaired water bodies across the United States. Given resource limitations, future monitoring efforts have to be hedged against the uncertainties in the monitored system, while taking into account existing knowledge. In that respect, we have developed a hierarchical spatiotemporal Bayesian model that can be used to optimize an existing monitoring network by retaining stations that provide the maximum amount of information, while identifying locations that would benefit from the addition of new stations. The model assumes the water quality parameters are adequately described by a joint matrix normal distribution. The adopted approach allows for a reduction in redundancies, while emphasizing information richness rather than data richness. The developed approach incorporates the concept of entropy to account for the associated uncertainties. Three different entropy-based criteria are adopted: total system entropy, chlorophyll-a standard violation entropy, and dissolved oxygen standard violation entropy. A multiple attribute decision making framework is adopted to integrate the competing design criteria and to generate a single optimal design. The approach is implemented on the water quality monitoring system of the Neuse River Estuary in North Carolina, USA. The model results indicate that the high priority monitoring areas identified by the total system entropy and the dissolved oxygen violation entropy criteria are largely coincident. The monitoring design based on the chlorophyll-a standard violation entropy proved to be less informative, given the low probabilities of violating the water quality standard in the estuary.

1. Introduction

[2] The collection of environmental data has the fundamental purpose of gaining a better understanding of the system we are monitoring. In an ideal world with no financial, temporal, or technical constraints, monitoring can be conducted at an infinite number of sites with instantaneous data collection and analysis. While recent advances in remote sensing, deployable sensors, and autonomous vertical profilers have reduced the above-mentioned constraints, monitoring at predefined locations remains by far the most common method for environmental data collection. Yet, the process of locating monitoring stations is often driven by convenience, making little use of more efficient network design methods [*Berthouex and Brown*, 2002; *Sanders et al.*, 1987; *Simeonov et al.*, 2003; *Strobl and Robillard*, 2008]. An exhaustive review of common approaches used in developing water quality networks is beyond the scope of this study; interested readers are encouraged to consult the review paper by *Strobl and Robillard* [2008]. *Mishra and Coulibaly* [2009] also present an exhaustive overview of recent developments in hydrometric networks.

[3] Many of the advances in the selection of monitoring locations have been brought about by developments in geostatistics [*Banerjee et al.*, 2003; *Christakos*, 2000]. Recognizing and accounting for both the spatial and temporal correlations of environmental variables provides a proper framework toward optimizing a monitoring network. However, acknowledging the spatiotemporal correlations through a model is insufficient by itself to guarantee a proper optimization. There is a need to couple that effort

---

[1]Nicholas School of the Environment, Duke University, Durham, North Carolina.

[2]Nicholas School is the Environmental Science and Policy Division, American University of Beirut, Beirut, Lebanon.

[3]Centre for Environmental Science and Engineering, Indian Institute of Technology Bombay, Mumbai, India.

[4]Department of Environmental Science, The University of Toledo, Ohio.

[5]Institute of Marine Sciences, University of North Carolina at Chapel Hill, Morehead City, North Carolina.

Corresponding author: I. Alameddine, American University of Beirut, Department of Civil and Environmental Engineering, Bliss street, PO Box 11-0236, Beirut, NA, Lebanon. (ia04@aub.edu.lb)

with an efficient approach that allows for the quantification of information (gain or loss) resulting from any proposed network redesign. The adoption of the concept of entropy, from information theory, allows for the quantification of system uncertainties over an appropriate probability distribution [*Caselton et al.*, 1992; *Christakos*, 2000; *Christakos and Li*, 1998]. The concept also lends itself toward assessing water quality standard violations. Assessing these violations has great relevance from a management perspective particularly with respect to the total maximum daily load (TMDL) program that entails the expenditure of significant resources (∼$ 17.3 million/year) to monitor more than 40,000 standard violations in around 20,000 impaired water bodies across the United States [*Environmental Protection Agency*, 2001; *National Research Council*, 2001].

[4] Entropy-based optimization methods have mostly been implemented towards redesigning air quality networks [*Ainslie et al.*, 2009; *Le and Zidek*, 2006; *Puangthongthub et al.*, 2007] and for optimizing flow and water level gauges [*Alfonso et al.*, 2010a, 2010b; *Li et al.*, 2012; *Markus et al.*, 2003]. Their adoption for redesigning water quality networks has been less common. Some studies have incorporated entropy in the design of water quality networks [*Harmancioglu and Alpaslan*, 1992; *Karamouz et al.*, 2009; *Ozkul et al.*, 2000]; however, most have fallen short of making full use of the spatiotemporal correlations in the data. Many of these studies had to discretize the underlying distribution of the variable of interest to simplify the calculation of entropy. Yet, discretizing the distribution on the water quality parameter may not achieve a unique design solution, as the estimated entropy values are dependent on the underlying discretization method. *LoBuglio et al.* [2007] were able to resolve this limitation by developing a Bayesian maximum entropy model that was capable of handling continuous distributions. Their model however, assumed a spatially homogenous and temporally stationary process as they attempted to optimize chlorophyll-a (Chl-a) monitoring in the Catawba River reservoir system in North Carolina.

[5] While assuming isotropic and stationary conditions may be valid in some cases, these assumptions are often hard to justify in dynamic coastal systems, such as estuaries. Riverine inputs, wind driven mixing, and saltwater influx lead to complex circulation patterns and make many estuarine systems anisotropic and nonstationary. Failing to properly account for the spatiotemporal correlations in the data can impede monitoring optimization in these complex water systems.

[6] In this paper, we explore the use of entropy as an information measure to properly quantify system uncertainties, while using a spatiotemporal hierarchal Bayesian model that is not restricted by either spatial isotropy or stationarity. Moreover, the adopted approach is not constrained towards optimizing a monitoring network based on a single water quality parameter nor on a particular criterion or attribute.

[7] We apply our developed model on the Neuse River Estuary in North Carolina to identify locations where our knowledge about the system is most limited given the existing monitoring program. Given that the methodology does not place any constraints on the random spatial fields assigned for the environmental variables of interest except

that they follow a joint matrix normal distribution, the proposed approach is particularly valuable to adopt in flow-complex water bodies. It should be noted that many environmental data are lognormally distributed; thus, log-transformation may be required.

[8] The proposed framework also incorporates a multiple attribute decision making (MADM) process, which allows for the integration of several competing design criteria to generate a single optimal design. To our knowledge, this is a novel approach toward assessing the adequacy of existing water quality monitoring networks and toward identifying vulnerable areas that would benefit most from additional monitoring given a set of competing design criteria.

[9] We describe the development of the Bayesian Hierarchal spatiotemporal model for predicting monthly averaged surface Chl-a and bottom dissolved oxygen (DO) concentrations, given the existing Neuse Estuary monitoring network. We then introduce the entropy-based optimization criteria that were adopted along with the analytical hierarchical process (AHP) that we implemented to weight and prioritize the different optimization criteria/attributes. We then present the optimization results for each design criteria and compare them with the final multicriteria based design. It is hoped that our work will be of use for both water quality monitoring agencies and policy makers.

2. Methods

2.1. Study Area and Data Description

[10] The Neuse River drains a 16,000 km^2 watershed. The river has its headwaters to the north of the city of Durham and travels approximately a distance of 443 km before discharging into an estuary located just below the city of New Bern. The estuary has been increasingly under pressure from anthropogenic activities in its contributing watershed as well as from climatic perturbations [*Paerl et al.*, 2006; *Paerl et al.*, 2009; *Paerl et al.*, 2010]. The estuary eventually connects to the Pamlico Sound (PS) after traveling around 78 km (Figure 1). The Neuse Estuary is the largest of the four major riverine tributaries feeding into the PS [*Paerl et al.*, 2007].

[11] The river and its associated estuary have experienced eutrophication with extensive algal blooms, fish kills, hypoxia and anoxia in the 1980s and 1990s [*Borsuk et al.*, 2003; *Paerl*, 1987; *Paerl et al.*, 1995; *Stow et al.*, 2003]. The estuary was listed on the 303(d) list of impaired water bodies [*Stow et al.*, 2003]. In 1998, the USEPA settled a lawsuit brought by the Neuse River Foundation, which required North Carolina to establish a TMDL for the nitrogen reaching the estuary. The TMDL was approved by the USEPA on August 26, 1999 [*NC Department of Environment and Natural Resources*, 1999]. Following the implementation of the TMDL program, Chl-a concentrations in the estuary have decreased and the frequency of standard violations (Chl-a ≥ 40 μg/L) have been significantly reduced. Similarly, bottom DO levels have since increased; yet they still drop below the 4 mg/L standard during the summer season (Figure 2b). Currently, many sections of the estuary have been delisted from the federal 303(d) list of impaired water bodies; nevertheless, around 16% of the total estuary area remains impaired [*Deamer*, 2009]. Given these changes in both mitigation and legislation,
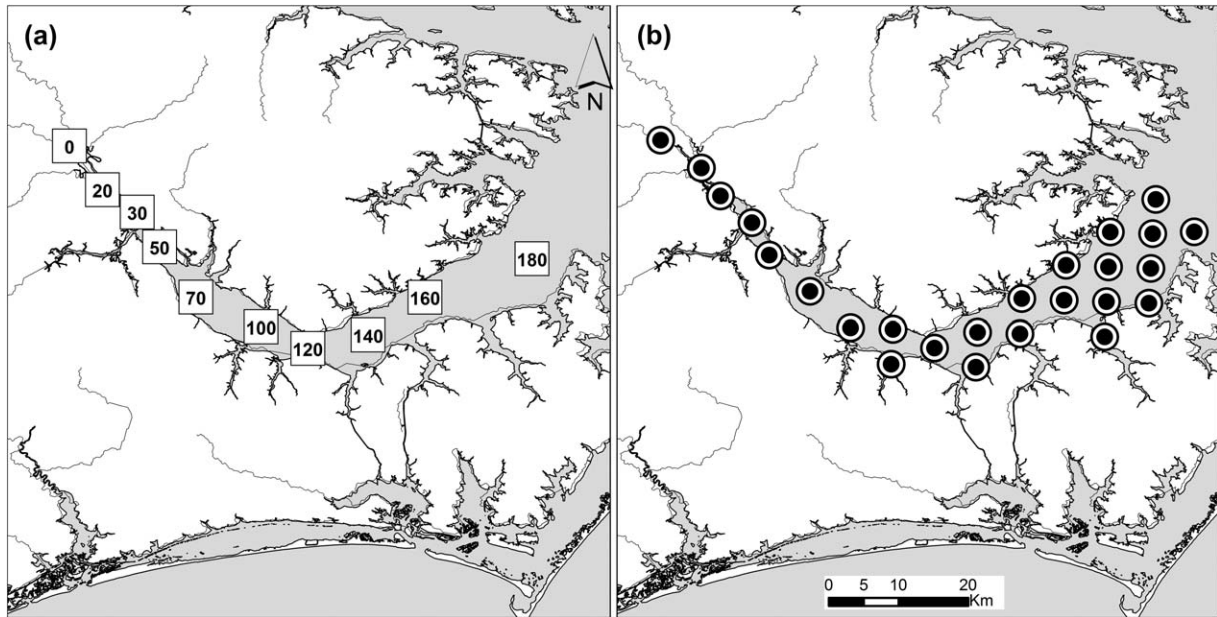
Figure 1. (a) Locations of the existing ModMon monitoring stations. Interstation separation distances range between 1.5 km (between stations 60 and 70) and 9.4 km (between stations 160 and 180), (b) the 25 potential locations generated from the 5 × 5 km representation of the Neuse Estuary.

reassessing the existing monitoring plan at this point to take into account these changes is constructive.

[12] Monthly averaged surface Chl-a and bottom DO concentrations were compiled from the ModMon program (http://www.unc.edu/ims/neuse/modmon) for the period between 2000 and 2005 [*Luettich et al.*, 2000a; *Valdes-Weaver et al.*, 2006]. Figure 1a shows the locations of the ModMon monitoring stations along the Neuse Estuary. Note that the existing monitoring stations are mostly placed equidistantly from each other. Such a design is usually the most appropriate in the absence of prior information on the system.

[13] To better characterize the study area, a 5 × 5 km grid was constructed taking into account the estuary's shape. The centroids of the pixels were then used as ungauged locations on which we were interested in quantifying prediction uncertainty. The generated grid yielded 25 potential locations (Figure 1b). We found that the selected 5 km resolution grid was the most optimal as it achieved a reasonable approximation of the irregular shape of the estuary with a limited number of pixels. While we could have selected a finer resolution, increasing the number of potential locations beyond the limits of the data (11 stations monitored over 5 years) can pose problems from a Bayesian computation perspective, as it becomes harder to guarantee that the predictive confidence intervals at the ungauged sites will remain simultaneously valid [*Le and Zidek*, 2006]. A simultaneously valid confidence interval ensures that the joint predictions at the ungauged sites simultaneously cover the specified confidence interval (e.g., 95%). The probability that all the predictions will simultaneously lie in their respective confidence intervals is lower than that which looks at the confidence interval for each prediction individually [*Le and Zidek*, 2006]. Note that in practical applications, all monitoring sites should also be selected in accordance with the recommendations

detailed in the National Field Manual for the Collection of Water-Quality Data [*Wilde*, 2005].

[14] Monthly, Chl-a concentrations were log-transformed to normalize the data. The use of log-transformation is a common practice when dealing with environmental data, which approximately follow a lognormal distribution [*Environmental Protection Agency*, 1994; *Murphy and Morrison*, 2002; *Ott*, 1995]. Bottom DO concentrations did not undergo any transformation.

[15] The Chl-a concentrations across the ModMon stations showed spatiotemporal patterns. Concentrations started out low in the upper section of the estuary before increasing downstream. They reached a maximum around the bend section (between station 120 and station 140 in Figure 1a) before decreasing as nutrient delivery dropped and salinity levels increased. These dynamics were consistent with Chl-a patterns previously documented for the Neuse Estuary [*Borsuk et al.*, 2004; *Paerl*, 2006; *Pinckney et al.*, 1998; *Qian et al.*, 2000]. The system also showed some seasonal dynamics with early spring and fall blooms and elevated Chl-a concentrations during the summer season [*Pinckney et al.*, 1998]. As expected, the winter season was the least productive (Figure 2a). As was previously observed by *Qian and Reckhow* [2007], monthly Chl-a levels in the estuary seldom exceed the set water quality standard of 40 μg/L (Figures 2a and 2b).

[16] Bottom DO levels, on the other hand, showed a pronounced temporal pattern with limited spatial structure (Figures 2c and 2d). DO levels in the estuary experienced a summer minima with the median values for June, July, and August all falling below the set 4 mg/L standard (Figure 2c). This drop was mainly due to increased water temperatures, less frequent vertical mixing, and increased bacterial activity in the sediment. These patterns were consistent with those described previously by *Borsuk et al.* [2001].
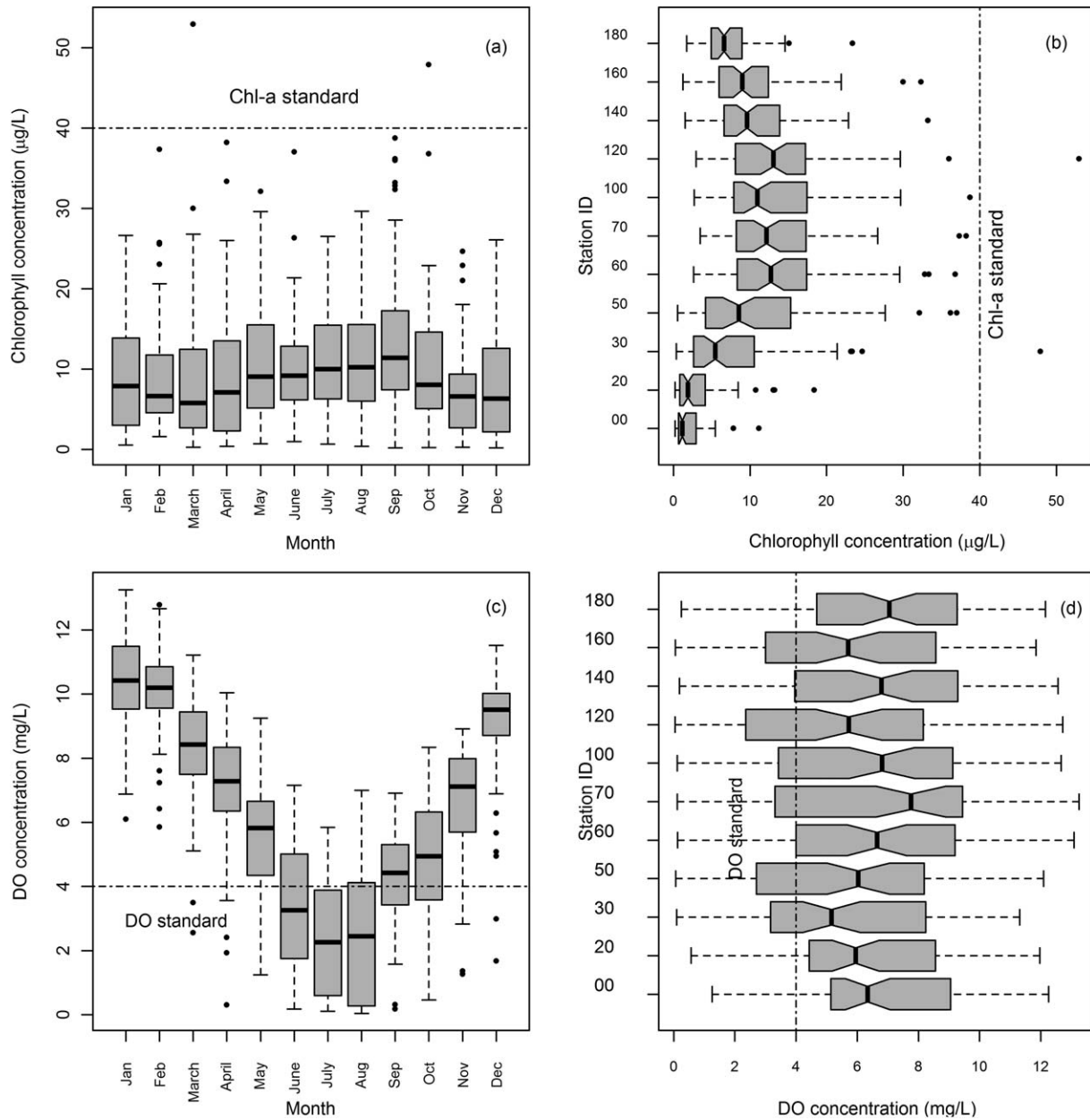
Figure 2. Variations in Chl-a concentrations in the Neuse Estuary by months (a) and across the monitoring stations (b). Variations in DO levels in the Neuse Estuary by months (c) and across monitoring stations (d). The dash-dotted lines represent the 40 μg/L and the 4 mg/L standards for Chl-a and bottom DO concentrations in North Carolina, respectively.

2.2. Sampson and Guttorp (SG) Method

[17] To deal with potential nonstationarity in the Neuse Estuary, the SG method was used. The SG-method is a nonparametric approach that can estimate the spatial covariance structure for a random field without assuming stationary [*Guttorp and Sampson*, 1994; *Guttorp et al.*, 1992; *Sampson and Guttorp*, 1992]. A 1-1 nonlinear smoothing mapping is first constructed from the geographic space (G-Space), where stationary is not assumed, to the dispersion space (D-space), where isotropy is assumed. The mapping process is conducted through an iterative algorithm, where the locations of the gauged locations are redistributes to generate a plane where the spatial dependency of the bivariate random field could be assumed isotropic. The algorithm is run for 1000 iterations; convergence is achieved once the difference between iterations becomes negligible (10^{-5}). Mapping between D-space and geographic space is made possible by means of a thin-plate spline [*Wahba and Wendelberger*, 1980]. The mapping function is then applied to any two locations in G-space. This allows for the mapping of the ungauged locations to D-space. Note that the SG method ensures that no spatial folding occurs in the mapping process through the selection of an appropriate smoothing parameter (λ). In this study, λ was set to 1. Several studies have shown that the model is not sensitive on the choice of λ [*Ainslie et al.*, 2009;

Le and Zidek, 2006; *Pollice and Jona Lasinio*, 2010]. An exponential semi-variogram was then fit using the D-space calculated distances and the observations at the gauged locations. The semi-variogram model was then used to estimate the dispersion between the ungauged sites and the gauged locations. This permitted extending the spatial covariance to the ungauged sites, resulting in the estimation of the spatial covariance matrix at all locations. Under the SG methodology, the spatial correlations were modeled by an isotropic exponential semivariogram that was fit using the interstation separation distances measured in a deformed plane termed the dispersion space (D-space) [*Guttorp and Sampson*, 1994; *Guttorp et al.*, 1992; *Sampson and Guttorp*, 1992].

2.3. Bayesian Hierarchal Model

[18] Following the mapping between G-space and D-space through the use of the SG method, a Bayesian hierarchical model was fit under D-space, where the isotropy assumption is respected. The adopted Bayesian hierarchical model jointly modeled the distribution on surface Chl-a concentrations (log transformed) and bottom DO levels in the Neuse Estuary as a joint matrix normal distribution. This allowed us to account for both the intervariable correlations and the observed spatiotemporal patterns (Figure 2). The model incorporated time varying covariates, which include year and month as categorical covariates, along with the average monthly water temperature in the Neuse Estuary as a continuous predictor. The decision to have monthly average water temperature as an additional predictor in the model stemmed from the fact that both surface Chl-a and bottom DO concentrations in the estuary were known to vary as a function of water temperatures [*Borsuk et al.*, 2004; *Borsuk et al.*, 2001]. These temporally varying covariates allowed the model to account for differences in the annual and monthly means. The incorporation of a high-frequency component (months) along with a long-term trend is a common approach when dealing with environmental time series [*Qian et al.*, 2000]. The use of temporal covariates within the model eliminated the need to detrend and deseason the data in a separate step and to account partially for temporal autocorrelations. This approach was shown to reduce spatial correlation leakage as described by *Le and Zidek* [2006].

[19] The two response variables were modeled through a bivariate random field that can be described by a joint matrix normal distribution (equation (1)). The mean of this matrix distribution is itself a matrix that can be expressed as a linear regression model that predicts the mean of the two environmental variables concurrently using a set of appropriate covariates (X).

$$MODEL:$$
$$Y|X, B, \sum \sim MVN(XB, I_t \otimes \sum) \quad (1)$$

$$PRIORS:$$
$$B|B_0 \sum, F^{-1} \sim MVN(B_0, F^{-1} \otimes \sum) \quad (2)$$

$$\sum |\Psi, \delta \sim GIW(\Psi, \delta) \quad (3)$$

where Y is an $(t \times 2n)$ dimensional matrix of the monthly mean concentrations of the two environmental variables under consideration at n sites over t time steps. n included both gauged and ungauged sites. X is a $(t \times k)$ dimensional matrix, where k is the number of temporally changing but spatially constant covariates. B is a $(k \times 2n)$ matrix of regression coefficients that are allowed to vary over sites [*Le and Zidek*, 2006; *Pollice and Jona Lasinio*, 2010]. $\sum$ $(np \times np)$ is the between sites/pollutant covariance matrix. $\sum$ can be partitioned over the gauged and ungauged sites using the Bartlett decomposition. $\sum$ was assigned a Generalized Wishart distribution (equation (3)) with a hypercovariance matrix Ψ, with the same dimensions as $\sum$, and δ degrees of freedom. F^{-1} denotes a matrix that rescales Σ to obtain the prior covariance matrix of β conditional on $\sum$ [*Ainslie et al.*, 2009]. As such, F^{-1} represents the amongst covariate variance component of β. $\otimes$ is the Kronecker product operation on two matrices and I_t is a $t \times t$ identity matrix.

[20] The regression coefficients matrix, B, was assigned a prior multivariate matrix normal distribution (equation (2)). The covariance between sites as well as the correlation between the two response variables was captured in the covariance matrix (Σ) (equation (1)). Σ is separable into two components namely, the between-variables covariance matrix that is fixed across space, and the between-site covariance matrix, which captures the spatial correlations. Σ was assigned a conjugate generalized inverted wishart (GIW) prior distribution (equation (2)). Since GIW is the conjugate prior for the covariance matrix of the matrix normal distribution, the posterior predictive distribution of the unobserved responses, conditional on the data and the hyperparameters, had a matric-t distribution. Note that the choice of the distributional families on the priors is a subjective process and may affect model inference. Yet, with well-identified parameters and large sample sizes, choosing reasonable prior distributions has minor effects on posterior inferences [*Gelman*, 2002].

[21] The defined priors on B and Σ have a set of hyperparameters that include B_0, Ψ, F^{-1}, and δ. While in a formal Bayesian methodology one would add an additional layer to the above hierarchy by assigning priors (often diffuse) to the hyper-parameters themselves, in this study we used empirical Bayes to define the hyper-distributions. Moreover, the decision to adopt an Empirical Bayesian approach was to reduce subjectivity that may arise from the definition of priors. Under the Empirical Bayesian approach, the data are used to determine the parameters of the priors by maximizing the marginal distribution of the observed data [*Bayarri and Berger*, 2004; *Carlin and Louis*, 2000]. This approach also improves computation and minimizes bias in the generated model posteriors [*Le and Zidek*, 2006]. Details concerning the assignment of the hyperdistributions are beyond the scope of this paper; they are discussed in depth by *Gelman* [2006], *Le and Zidek* [1994], and *Van Dongen* [2006]. The use of Empirical Bayes in water quality assessment is common, particularly when dealing with a hierarchal or nested data [*Butcher et al.*, 2003; *Canham et al.*, 2003; *Reckhow*, 1996; *Solow and Gaines*, 1995]. The defined hierarchal Bayesian model (equations ((1)–(3))), leads to a conditional joint predictive distribution at the ungauged locations that is a matrix-Student t-distribution. A more complete overview of the

model specification is provided by *Le and Zidek* [2006] and is therefore not repeated here.

2.4. Entropy

[22] Entropy (Shannon's entropy) is a measure of the amount of information that is missing before learning the occurrence of an event [*Caselton et al.*, 1992]. It describes the uncertainty associated with a given probability distribution. Entropy for the continuous bivariate random field is defined by $H(Y) = E\left[-\frac{Log f(Y)}{h(Y)}\right]$, where E is the expectation, $f(Y)$ is the joint probability distribution for Chl-a concentrations and bottom DO levels and $h(Y)$ is a measure that represents complete ignorance. $h(Y)$ is included to ensure that entropy is invariant under affine transformation of the predictors (X) [*Jaynes*, 1963; *Le and Zidek*, 1994]. Here, we assumed $h(Y)$ to be identically 1. We used entropy to quantify model uncertainty, which was used to guide monitoring optimization in the Neuse Estuary. Three different entropy-based criteria were adopted, namely total system entropy, Chl-a standard violation entropy, and DO standard violation entropy.

2.4.1. Total System Entropy

[23] The optimization of the monitoring design based on total system entropy focuses on minimizing residual entropy following data collection [*Caselton et al.*, 1992; *Le and Zidek*, 1994, 2006]. This entails choosing to monitor locations that have maximum values of entropy given the existing data. Since the entropy of a multivariate Gaussian distribution is directly proportional to the log determinant of the covariance (refer to the supporting information material), locations with the largest log determinant need to be monitored. These stations hold the maximum amount of latent information. Monitoring at these locations guarantees that the uncertainty in model parameters and in the predictive distributions at the rest of the ungauged locations are minimized [*Le and Zidek*, 2006]. Since the posterior predictive distributions depend on the model parameters, reducing the uncertainty of these model parameters was also a key objective to be incorporated in optimizing the network [*Caselton et al.*, 1992; *Le and Zidek*, 2006]. The optimization focused on selecting the locations whose entropy was greatest. Monitoring those locations maximizes system information [*Ainslie et al.*, 2009]. This was guaranteed by the fact that the total a priori entropy of the system is fixed [*Le and Zidek*, 1994].

2.4.2. Standard Violation Entropy

[24] While the system's entropy is an adequate criterion when it comes to choosing the most appropriate sites for locating additional monitoring stations, it did not explicitly account for violations in the relevant water quality standards. To account for these violations, we accounted for violation probabilities. The Chl-a standard in North Carolina is 40 μg/L (maximum), while the bottom DO standard is 4 mg/L (minimum). We calculated the probability of standards violation over time and across all locations to identify locations that had the highest violation probabilities.

[25] Violation probabilities can be useful for designing a network and for TMDL nonattainment listing [*LoBuglio et al.*, 2007]; yet, they do not necessarily guarantee the most efficient selection of monitoring sites. This is because

they are biased towards the selection of locations that have the highest probability of violations. From an information theory perspective, the locations that are in need of monitoring are those whose compliance status we are most uncertain about. These locations were identified by calculating their violation entropies. Note that for low probabilities of violation both probability and entropy based designs lead to similar solutions. However, the two methods diverge in their conclusions when the violation probabilities increase. Locations with high probabilities of violation will have low corresponding entropies. The latter reaches its maximum when the probability of violation is 50%. We argue that using violation entropy is more relevant both from an information and management perspective.

[26] Standard violation entropy was calculated through model simulation. A thousand joint samples were drawn from the posterior predictive distribution of the bivariate random field across the set of proposed locations over a period of 6 years. For each time-step (t), we calculated the water quality standard violation probabilities (P_{DO} and P_{chl}) at the 25 ungauged locations. The violation probabilities were estimated as the fraction of observations violating a given standard (equations (4) and (5)). Our adoption of a simulation-based assessment avoided integration over the high dimensional space of the joint bivariate random field.

$$P_{chl_{i,t}} = \frac{\sum_{j=1}^{1000} I\left(Chla_{i,t,j} \geq 40\,\mu g/L\right)}{1000} \quad (4)$$

$$P_{DO_{i,t}} = \frac{\sum_{j=1}^{1000} I\left(DO_{i,t,j} \leq 4\,mg/L\right)}{1000} \quad (5)$$

where $Chla_{i,t,j}$ is the chlorophyll concentration at site i, and time t, $P_{Chla_{i,t}}$ is the associated probability of standard violation. Similarly, $DO_{i,t,j}$ is the bottom DO level at site i, and time t, $P_{DO_{i,t}}$ is the associated probability of standard violation at that site for that time period. I is an indicator function that returns 1 if the condition is satisfied and zero otherwise; j represents the number of the simulation.

[27] Given that standard violation is a Bernoulli process, we calculated the violation entropy for each time-step using equation (6). Since the predictions at time t are largely independent of $t+1$ and $t-1$ given the model parameters, the joint entropy for each potential monitoring location across time can be estimated through equation (7).

$$H(X_t) = -p_t \times \log_2 p_t - (1 - p_t) * \log_2(1 - p_t) \quad (6)$$

$$H(X_1, \ldots, X_t) = H(X_1) + \ldots + H(X_t) \, iff \, X_1, \ldots, X_t \, are \perp \quad (7)$$

where p_t represents the probability of standard violation at time t at a given location. Note that the independence assumption may be violated in the event that significant temporal variability remains unexplained by the model. Choosing the locations with the largest standard violation entropy ensured that priority was given to sites where our knowledge on standard violations was most uncertain. To account for the two water quality standards, we generated

an optimized design based on each of the two standards.

2.7. The AHP Framework

[28] Each of the three criteria (total system entropy, Chl-a standard violation entropy, DO standard violation entropy) resulted in a different solution. Therefore, an efficient approach was needed to weight and incorporate the different design elements from the three criteria so as to generate a single optimal solution. This was achieved by adopting a MADM process that weighs the three design attributes or optimization criteria. The details of the adopted MADM approach are presented in the online supporting information material.

[29] Similarly, the ranking of the 25 potential monitoring sites given each of the three criteria was achieved through a MADM process. We adopted the AHP approach for MADM. AHP is an efficient decision analysis tool that can be used to rank a finite number of options or alternatives based on a set of multiple attributes [*Saaty*, 1987, 1977, 1986, 1990, 1994, 2005; *Stein and Mizzi*, 2007; *Yoon and Hwang*, 1995]. This is achieved through subjective pairwise comparisons. AHP is one of the most widely used MADM tools [*French et al.*, 2009; *Marshall and Oliver*, 1995; *Vaidya and Kumar*, 2006]. Several AHP procedures have been developed over the years, with conventional AHP being mostly used when a single decision-maker is involved.

[30] Advances in AHP have focused in expanding the capabilities of the procedure to handle group decisions and its associated uncertainties. Multiplicative AHP is one of these advances [*Barzilai et al.*, 1987; *Huang et al.*, 2009; *Lootsma*, 1988, 1993; *Van Den Honert and Lootsma*, 1997]. We have applied both conventional and multiplicative AHP to prioritize the selection of monitoring stations and to verify the stability of the obtained results by comparing the results from the two techniques. The results did not show any sensitivity towards the adopted AHP procedure, implying a stable solution.

[31] The relative importance of the three monitoring optimization criteria was assessed by eliciting the opinion of four water quality experts from North Carolina. The adopted questionnaire is presented in the online supporting information material. The results from each expert were equally weighted and combined. This implies that our pairwise interexpert matrix was populated with a Saaty score of 1.

[32] A similar pairwise comparison matrix (PCM) approach was adopted to rank the 25 ungauged locations based on each of the three criteria. However, in this case the PCMs were numerically derived from modeled entropy values calculated at each of the 25 locations. Interstation entropy ratios were determined and normalized. Ratios ≥ 1 were then linearly interpolated to the Saaty scale. Their transpose in the 25×25 comparison matrix would thus be assigned the reciprocal value of the Saaty score of their respective transpose [*Harker and Vargas*, 1987; *Saaty*, 1986, 1990, 1994].

[33] Consistency tests on the PCMs were conducted through the calculation of the consistency ratio (CR) [*Saaty*, 1990; *Stein and Mizzi*, 2007]. This step ensured that the priorities provided by the four experts were inter-nally consistent. A detailed account of the adopted AHP process is presented in the supporting information material.

3. Results

[34] The model was able to capture both the long-term as well as the seasonal patterns observed for surface Chl-a and bottom DO concentrations. The results indicated that on average the Chl-a concentrations have decreased post 2000, with the median concentration dropping from 13.1 µg/L in 2000 to 8.8 µg/L in 2005. Bottom DO concentrations, on the other hand, were found to have increased during the same period, with the largest increase occurring in 2005. The observed improvements in the water quality of the Neuse Estuary were probably associated with the implementation of the nitrogen TMDL program in the Neuse River basin that limited flow-driven nitrogen delivery to the estuary [*Alameddine et al.*, 2011].

[35] Observed seasonal patterns for surface Chl-a levels (Figure 2a) were accounted for by the model coefficients on the months. The highest mean monthly concentrations occurred in September. Yet, some of the model coefficients for the months were not statistically different from each other. This was expected given the patterns observed in Figure 2. The seasonality in bottom DO levels (Figure 2c) was mostly accounted for by the seasonal variations in water temperatures. This strong negative linear relationship between bottom DO concentrations and the water column temperature measurements has been previously documented by *Borsuk et al.* [2001] for the Neuse Estuary.

[36] The correlation between bottom DO levels and surface Chl-a concentrations was found to be weakly negative ($\rho = -0.13$). On the other hand, the spatial correlations between the existing stations in ModMon were captured in the inter-station correlation matrix. As expected, stations that were spatially closer together had higher correlations (Table 1). Yet, the magnitudes of these correlations were not constant across space. We observed that the spatial correlations between the stations and their immediate neighbors in the upper part of the estuary became weaker as we moved downstream. This was probably due to changes in the riverine flow dynamics along this section of the estuary. Note that the scale of the spatial correlations increased again past station 70 (Table 1).

[37] The lack of uniformity in the spatial correlations in the Neuse Estuary system did not allow the use of ordinary krigging, which assumes second-order stationary and isotropy [*Banerjee et al.*, 2003; *Qian*, 1997]. As such, the SG method was adopted. The deformation results for the Neuse Estuary did not show drastic deviations from the original geographic space (supporting information material). The results showed that Stations "60" and "70" appeared to be more far removed from Stations "50" than what Euclidian separation distances alone would indicate. This highlights differences between the upper and middle sections of the estuary.

3.1. Network Optimization Based on Total System Entropy

[38] The optimization based on total system entropy proceeded by identifying the locations that would add the most to our knowledge about the system. In this study, we

Table 1. The Marginal Correlation Matrix Between the Currently Monitored Stations in the ModMon Program[a]

Station	0	20	30	50	60	70	100	120	140	160	180
0	1	0.70	0.18	0.11	−0.08	0.04	−0.07	−0.03	0.00	0.09	0.20
20		1	0.56	0.26	−0.06	−0.01	−0.18	−0.15	−0.13	0.01	0.13
30			1	0.55	0.15	−0.02	−0.09	−0.06	−0.10	−0.07	0.02
50				1	0.44	0.36	0.16	0.19	0.02	−0.10	−0.03
60					1	0.70	0.41	0.19	0.12	−0.04	0.11
70						1	0.54	0.40	0.24	0.19	0.10
100							1	0.60	0.42	0.18	0.16
120								1	0.65	0.48	0.25
140									1	0.61	0.68
160										1	0.61
180											1

[a]Station 0 is located toward the beginning (river section) of the estuary, while Station 180 is the last station currently monitored before the Neuse Estuary opens to PS (Figure 1). Gray shaded cells indicate correlations > then 0.5.

limited our analysis to the identification of a single station. Yet, the same methodology can be expanded to explore the addition of multiple stations. Clearly from an entropy perspective, the most suitable station to add would be the one whose future monitoring is expected to carry the most information for the system as a whole. This entails reducing both the predictive uncertainty for Chl-a and DO levels in the Neuse Estuary, as well as decreasing the model parameter uncertainties. This was achieved by looking for a location with the largest log determinant computed from the residual covariance matrix conditional on observed data [*Le and Zidek*, 1994, 2006; *Le et al*., 1997].

[39] Figure 3 shows the relative magnitude of the entropy measure for each of the 25 proposed sites. Of these sites, monitoring at E1 would add the most information to the system. The choice of E1, which is located towards the lower Neuse Estuary, was not surprising given that the station is located the furthest away from the Neuse flow centerline. Moreover, a closer examination of the estimated covariance matrix for the 25 ungauged locations showed higher model uncertainties associated with that location. Adding a monitoring station at E1 would give us a better understanding of surface Chl-a and bottom DO dynamics in that section of the estuary and add the most information to the system as a whole. Note that location E2, which had the second highest entropy, is also located away from central flow line. The location with the largest entropy, but still located on the main flow path of the estuary, was found to be located in E3 (Figure 3). The selection of E3 was expected given that our initial assessment of the correlations between existing stations revealed that the spatial correlation between Station "50" on one hand and Stations "60" and "70" on the other were lower than expected (Table 1). That section of the estuary was probably the section where changes in riverine flow, nutrient loadings, and salinity levels were the largest.

### 3.2. Network Optimization Based on Standard Violation Entropy

[40] With respect to Chl-a standard violation, site CHL1E was associated with the largest violation entropy (Figure 4b). Note that the second (CHL2E) and third (CHL3E) locations with highest Chl-a violation entropies were located in the vicinity of CHL1E. This spatial pattern indicated that the section of the Neuse Estuary that stretches between Stations "30" and "70" was associated

with the largest amount of uncertainty with respect to Chl-a standard compliance. This is primarily due to the elevated Chl-a concentrations observed in that section of the estuary as a result of nutrient delivery and favorable physical conditions (Figure 2). Nevertheless, the model results indicated that there was a very small probability of exceeding the Chl-a standard across the 25 locations in the Neuse Estuary (Figure 4a). The predicted median probability of standard violation across the 25 ungauged locations over the 6 years of analysis did not exceed 2%. This is not surprising given that between 2000 and 2005, the standard was only exceeded twice [*Qian and Reckhow*, 2007]. Under low violation probabilities, the corresponding exceedance entropies were low as well. Therefore the optimization results based on either probability or violation entropy produced comparable results. Discrepancies observed between Figures 4a and 4b are largely attributed to the fact that violation probability was calculated for the entire time period (equation (4)), while the violation entropy was summed over smaller time-steps (equation (7)).
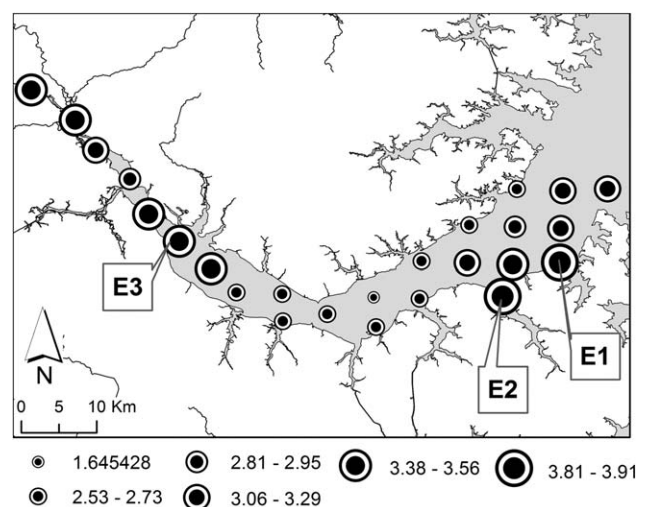
Figure 3. The locations of the proposed 25 locations are shown in the map. The relative size of each symbol is proportional to the computed entropy for that station. E1 is the station with the largest system entropy. E2 and E3 are second and third in terms of entropy, respectively.
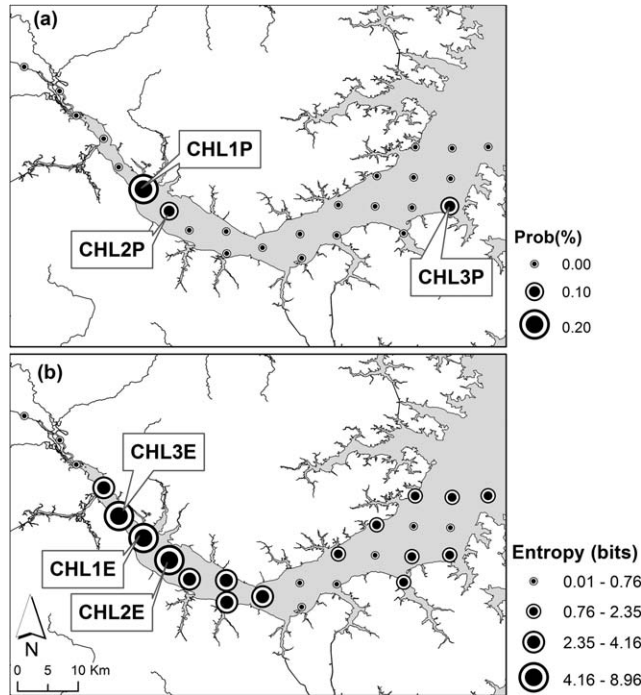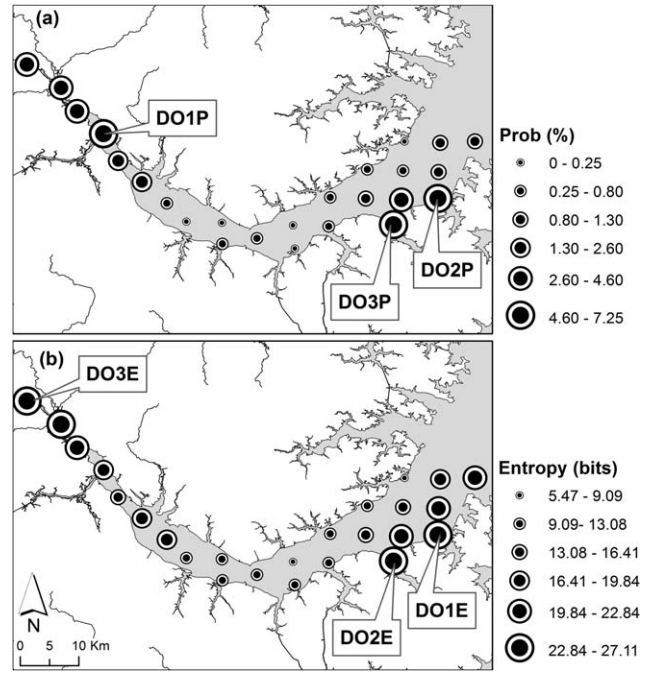
Figure 4. (a) Chl-a standard exceedance probability based on the 40 µg/L bottom standard at the 25 proposed locations. The size of each point is proportional to its exceedance probability; (b) standard violation entropy for the 25 proposed locations. The size of each point is proportional to its standard violation entropy value.
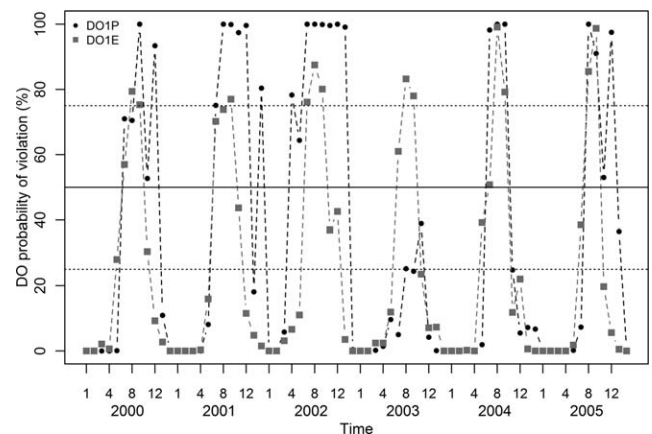

Figure 5. (a) DO standard violation probability based on the 4 mg/L bottom DO standard at the 25 proposed locations. The size of each point is proportional to its violation probability; (b) standard violation entropy for each of the 25 proposed locations. The size of each point is proportional to its standard violation entropy value.

ordered seasonal pattern for bottom DO, which resulted in their high violation entropy.

3.3. AHP Based Results: A Compromise Solution

[43] The multiplicative AHP approach was used to find a compromise solution between the three competing optimization designs. The expert panel intercriteria comparison resulted in prioritizing the three design criteria. The total

[41] For bottom DO concentrations, the same approach was adopted. Figure 5 compares the optimization results that are based on DO standard violation probability with those based on the violation entropy at the 25 proposed locations. Given that bottom DO levels often dropped below 4 mg/L, the entropy optimization (Figure 5b) was significantly different from that generated based on violation probabilities (Figure 5a). The differences were compounded by the strong seasonality that DO levels exhibited in the Neuse estuary (Figure 2c).

[42] At many stations, the violation probabilities for bottom DO showed a strong seasonal cycle, with violation probabilities around 0% for the months when the water temperatures in the estuary were low and violation probabilities around 100% for summer and early fall months when temperatures were high. Adopting a design based on probability of violation will thus be biased towards selecting stations that had very strong and distinct seasonal cycles with consistent violations all across the summer and fall seasons. However, the entropy based design will be more predisposed to select stations that exhibited less predictable seasonal patterns. This is clearly seen in Figure 6, which compares the violation probabilities across time for station DO1P, which had the highest violation probability, and station DO1E that had the largest standard violation entropy. For DO1P, the temporal variability in DO standard violation was either 0 or 100%. Meanwhile, the DO standard violation probabilities at DO1E ranged between 30 and 80% (Figure 3). Similarly, DO2E and DO3E showed a dis-

Figure 6. The probabilities of violating the bottom DO standard of 4 mg/L at the two locations DO1P and DO1E across time. The former is associated with the largest violation probability, while the latter is associated with the largest DO violation entropy. Note that x-axis shows the months and years.
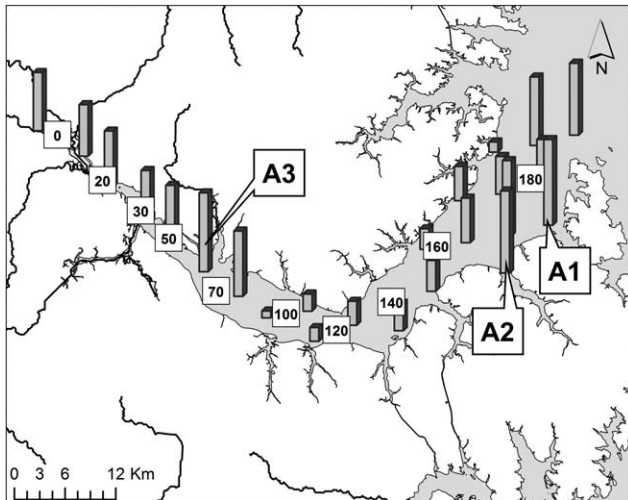
Figure 7. The relative importance of monitoring at the 25 proposed locations is reflected in the height of the associated vertical bars. The bar heights range from 1 to 25. The southern shoreline section that stretches between stations 160 and 180 has the highest values. The ranking is based on the three criteria we considered namely, total system entropy, Chl-a standard violation entropy, and DO standard violation entropy.

system entropy based optimization design received a 75% overall weight, the Chl-a standard-violation entropy design was assigned a 16% overall weight, and the bottom DO standard-violation entropy design was assigned the remaining 9%. The CR of the aggregated PCM for the panel of four experts was found to be 0.053, which is <0.10 threshold level defined by *Saaty* [*Saaty*, 1990; *Stein and Mizzi*, 2007]. This indicated a consistent judgment. Similarly, the 25 × 25 PCM matrices that were constructed for intersite comparisons had CR values below the Saaty score threshold (CR = 0.011 for total system entropy, CR = 0.014 for Chl-a standard violation entropy, and CR = 0.008 for DO standard violation entropy). This indicated consistency in derivation.

[44] The final ranking of the 25 locations based on the three criteria were computed by multiplying the expert priority matrix by the intersite priority matrices for the three attributes. The final optimization results based on the three

criteria are shown in Figure 7. It is apparent that the southeastern shoreline of the Neuse Estuary, which stretches between stations 160 and 180, is the section where our existing information is most limited. This section of the estuary was identified both based on total system entropy and the DO violation criterion. Moreover, given the priorities that the experts placed on each of the three criteria, the final design was heavily weighted by the total system entropy-based design.

[45] However, the locations just before the Neuse Estuary bend (between stations 100 and 140) were associated with the lowest monitoring priority; this indicates that our knowledge of Chl-a and DO dynamics in that section is relatively certain given the current monitoring program. This is supported by the work of *Luettich et al.* [2000b], who showed that this section of the estuary has very predictable vertical stratification dynamics. Moreover, this area has low standard violations entropies.

3.4. Model Cross-Validation

[46] A leave-one-out cross-validation was conducted by removing one station at a time and using the other 10 to predict the concentrations over time. Table 2 shows the results of the cross-validation whereby the temporally averaged predicted DO and the logarithm of chlorophyll concentrations at each of the omitted stations are compared to the observed temporally averaged concentrations at the removed station. The results indicate that the model performed reasonably well and did not show large biases. Moreover, the 95% prediction confidence intervals indicate that the model prediction errors seem to appropriately bracket the observed variability in the data (supporting information material). Note that removing Station "00" (the first station in the estuary where the river meets the system) resulted in predictions that were subpar as compared to the rest of the stations. Many of the observed chlorophyll data at Station "00" fell outside the 95% credible intervals predicted by the model. This is to be expected given the difficulty of extrapolating the spatial covariance matrix to an edge station, where the physical environment is largely different (shallower, higher velocity, lower salinity, etc).

4. Discussion

[47] Our proposed monitoring optimization framework allows for multicriteria optimization by incorporated a

Table 2. Leave-One Out Cross-Validation Results Generated by Removing One Station at a Time and Using the Other 10 to Predict Concentrations Over Time

Station	Observed mean log-transformed chlorophyll (μg/L)	Predicted mean log-transformed chlorophyll (μg/L)	Observed mean DO (mg/L)	Predicted mean DO (mg/L)
0	0.34	1.47	7.00	6.11
20	0.62	0.90	6.25	6.40
30	1.66	1.56	5.37	5.96
50	2.06	1.47	5.46	6.60
60	2.48	2.39	6.53	6.50
70	2.48	2.44	6.65	6.48
100	2.45	2.40	6.34	5.89
120	2.50	2.27	5.46	6.41
140	2.24	2.23	6.53	5.74
160	2.12	2.09	5.82	6.68
180	1.85	1.92	6.90	6.19

MSE: 0.16; RMSE: 0.40; NRMSD: 0.19; PBIAS (%): −1.64; MSE: 0.50; RMSE: 0.70; NRMSD: 0.43; PBIAS (%): −0.96.
The reported values are the temporally averaged observed and predicted values, also shown are common metrics used to assess model accuracy.

MADM component that permits different water quality experts to weigh-in and give their perspective on the relative importance of different optimization criteria. Moreover, the adopted framework is probabilistic in nature, which allows it to transparently account and propagate the uncertainties both in data and in model parameters. The model formulation did not place any limitations on the spatiotemporal field (stationarity or isotropy); an advantage that is particularly important in modeling dynamic water bodies (estuaries, coastal waters, dammed rivers, current driven waters, etc). Yet, the model assumes that the environmental variables can be properly modeled by a joint matrix normal distribution. To satisfy this assumption variable transformation may be required. As illustrated in this study, the framework was used to assess the existing water quality monitoring network in the Neuse Estuary based on multiple design criteria. We were able to identify the areas with maximum uncertainties and that would benefit most from future monitoring. The adopted methodology is flexible and can be easily adapted towards identifying redundant stations or toward replacing one (or more) of the existing stations with another locations based on the system's informational content. This can be achieved by iteratively dropping a single (or multiple) station and then running the same optimization algorithm, while treating the dropped station(s) as an additional station amongst the set of "new" stations being considered.

[48] Our results highlighted the differences between a probability and an entropy-based design. The results highlighted the advantages of adopting entropy as a monitoring design criterion. We think that the developed framework is a valuable tool for assisting scientists and managers in optimizing their monitoring efforts in impaired waters that are listed under section 303(d) of the Clean Water Act [*Environmental Protection Agency*, 2001; *National Research Council*, 2001].

[49] The optimization of a monitoring network should be coupled with a cost analysis. While our methodology did not explicitly account for cost, we assumed that the cost of monitoring at any locations was identical and represented an equal fraction of the total operational cost of the program. This assumption may not hold true from an operational stand-point, since the costs associated with the addition of a station may be nonlinear; however, it is still adequate for our purposes. More elaborate cost functions can also be incorporated within our developed framework if the need arises. Incorporating costs while accounting for uncertainty is an application of statistical decision theory [*Berger*, 1985; *Borsuk*, 2001].

[50] Another implicit assumption in our methodology was that information across the estuary is equally valuable. This might not be true in some cases, where certain areas may have a higher informational value. Such locations include shell-fishing areas, recreational beaches, and ecologically sensitive environments. Under such cases, an approach similar to the one adopted by *Puangthongthub et al.* [2007] can be incorporated within the modeling framework.

References

Ainslie, B., C. Reuten, D. G. Steyn, N. D. Le , and J. V. Zidek (2009), Application of an entropy-based Bayesian optimization technique to the redesign of an existing monitoring network for single air pollutants, *J. Environ. Manag.*, *90*, 2715–2729.

Alameddine, I., S. S. Qian, and K. H. Reckhow (2011), A Bayesian changepoint-threshold model to examine the effect of TMDL implementation on the flow-nitrogen concentration relationship in the Neuse River basin, *Water Res.*, *45*, 51–62.

Alfonso, L., A. Lobbrecht, and R. Price (2010a), Information theory-based approach for location of monitoring water level gauges in polders, *Water Resour. Res.*, *46*, W03528.

Alfonso, L., A. Lobbrecht, and R. Price (2010b), Optimization of water level monitoring network in polder systems using information theory, *Water Resour. Res.*, *46*, W12553.

Banerjee, S., A. E. Gelfand, and B. P. Carlin (2003), *Hierarchical Modeling and Analysis for Spatial Data*, Chapman and Hall/CRC, Boca Raton, Fla.

Barzilai, J., W. D. Cook, and B. Golany (1987), Consistent weights for judgements matrices of the relative importance of alternatives, *Oper. Res. Lett.*, *6*, 131–134.

Bayarri, M. J. and J. O. Berger (2004), The interplay of Bayesian and frequentist analysis, *Stat. Sci.*, *19*, 58–80.

Berger, J. O. (1985), *Statistical Decision Theory and Bayesian Analysis*, 2nd ed., Springer-Verlag, New York.

Berthouex, M. P. and L. C. Brown (2002), *Statistics for Environmental Engineers*, CRC, Boca Raton, Florida.

Borsuk, M. E. (2001), *A graphical probability network model to support water quality decision making for the Neuse River Estuary*, 267 pp, Duke University, Durham, North Carolina.

Borsuk, M. E., C. A. Stow, R. A. Luettich, H. W. Paerl, and J. L. Pinckney (2001), Modelling oxygen dynamics in an intermittently stratified estuary: Estimation of process rates using field data, *Estuar. Coast. Shelf Sci.*, *52*, 33–49.

Borsuk, M. E., C. A. Stow, and K. H. Reckhow (2003), Integrated approach to total maximum daily load development for neuse river estuary using Bayesian probability network model (Neu-BERN), *J. Water Resour. Plann. Manage.*, *129*, 271.

Borsuk, M. E., C. A. Stow, and K. H. Reckhow (2004), Confounding effect of flow on estuarine response to nitrogen loading, *J. Environ. Eng.*, *130*, 605–614.

Butcher, J. B., E. Thirolle, E. Booth, and A. Rooker (2003), *Estimating Limited-Data Urban Bacterial TMDLs Using Empirical Bayes Regionalization*, ASCE, Philadelphia, Pennsylvania.

Canham, C. D. W., J. Cole, and W. K. Lauenroth (Eds.) (2003), *Models in ecosystem science*, Princeton University Press, Princeton.

Carlin, B. P. and T. A. Louis (2000), *Bayes and Empirical Bayes Methods for Data Analysis*, 2nd ed., Chapman & Hall/CRC, Boca Raton.

Caselton, W. F., L. Kan, and J. Zidek (1992), Quality data networks that minimize entropy, in *Statistics in the Environmental & Earth Sciences*, edited by A. T. Walden and P. Guttorp, pp. 10–38, E. Arnold, London.

Christakos, G. (2000), *Modern Spatiotemporal Geostatistics*, Oxford University Press, New York.

Christakos, G. and X. Li (1998), Bayesian maximum entropy analysis and mapping: A farewell to kriging estimators?, *Math. Geol.*, *30*, 435–462.

Deamer, N. (2009), Neuse river basinwide water quality plan*Rep.*, NC Department of Environment and Natural Resources: Division of Water Quality, Planning Section – Basinwide Planning Unit, Raleigh, NC.

Environmental Protection Agency (1994), Statistical Training Course on Ground Water Monitoring Data Analysis Report, pp. 196, Washington, DC.

Environmental Protection Agency (2001), The National Costs of the Total Maximum Daily Load Program (Draft Report), pp. 51, United States Environmental Protection Agency, Washington, D.C.

French, S., J. Maule, N. Papamichail, and E. Corporation (2009), *Decision Behaviour, Analysis and Support*, Cambridge University Press, New York.

Gelman, A. (2002), Prior distribution, in *Encyclopedia of Environmetrics*, edited by A. H. El-Shaarawi and W. W. Piegorsch, pp. 1634–1637, Wiley, Chichester.

Gelman, A. (2006), Prior distributions for variance parameters in hierarchical models, *Bayesian Anal.*, *1*, 515–533.

Guttorp, P. and P. D. Sampson (1994), Methods for estimating heterogeneous spatial covariance functions with environmental applications, *Handbook Stat.*, *12*, 661–689.

Guttorp, P., P. D. Sampson, and K. Newman (1992), Nonparametric estimation of spatial covariance with application to monitoring network evaluation, in *Statistics in the Environmental & Earth Sciences*, edited by A. T. Walden and P. Guttorp, pp. 39–51, E. Arnold, London.

Harker, P. T. and L. G. Vargas (1987), The Theory of Ratio Scale Estimation: Saaty's Analytic Hierarchy Process, *Manag. Sci.*, *33*, 1383–1403.

Harmancioglu, N. B. and N. Alpaslan (1992), Water quality monitoring network design: a problem of multi-objective decision making, *J. Am. Water Resour. Assoc.*, *28*, 179–192.

Huang, Y. S., J. T. Liao, and Z. L. Lin (2009), A study on aggregation of group decisions, *Syst. Res. Behav. Sci.*, *26*, 445–454.

Jaynes, E. (1963), Information theory and statistical mechanics, in *Statistical Physics*, edited by K. W. Ford, pp. 181–218, Benjamin, New York.

Karamouz, M., A. Nokhandan, R. Kerachian, and Č. Maksimovic (2009), Design of on-line river water quality monitoring systems using the entropy theory: A case study, *Environ. Monit. Assess.*, *155*, 63–81.

Le, N. D. and J. V. Zidek (1994), Recent advances in statistics and probability. *Proceedings of the 4th International Meeting of Statistics in the Basque Country*, edited by J. P. Vilaplana and M. L. Puri, pp. 191–206, VSP, Utrecht, The Netherlands.

Le, N. D. and J. V. Zidek (2006), *Statistical Analysis of Environmental Space-Time Processes*, Springer, New York.

Le, N. D., W. Sun, and J. V. Zidek (1997), Bayesian multivariate spatial interpolation with data missing by design, *J. R. Stat. Soc: Ser. B*, *59*, 501–510.

Li, C., V. P. Singh, and A. K. Mishra (2012), Entropy theory-based criterion for hydrometric network evaluation and design: Maximum information minimum redundancy, *Water Resour. Res.*, *48*, W05521.

LoBuglio, J. N., G. W. Characklis, and M. L. Serre (2007), Cost-effective water quality assessment through the integration of monitoring data and modeling results, *Water Resour. Res.*, *43*, W03435.

Lootsma, F. A. (1988), Numerical scaling of human judgement in pairwise-comparison methods for fuzzy multi-criteria decision analysis, in *Mathematical Models for Decision Support*, edited by G. Mitra, pp. 57–88, Springer-Verlag, Berlin.

Lootsma, F. A. (1993), Scale sensitivity in the multiplicative AHP and SMART, *J. Multicriteria Decis. Anal.*, *2*, 87–110.

Luettich, R. A., J. E. McNinch, H. W. Paerl, C. H. Peterson, J. T. Wells, M. Alperin, C. S. Martens, and J. L. Pinckney (2000a), Neuse River Estuary modeling and monitoring project stage 1: hydrography and circulation, water column nutrients and productivity, sedimentary processes and benthic-pelagic coupling Report, pp. 172, Water Resources Research Institute of the University of North Carolina, Raleigh, NC.

Luettich, R. A., J. E. McNinch, H. W. Paerl, C. H. Peterson, J. T. Wells, M. Alperin, C. S. Martens, and J. L. Pinckney (2000b), *Neuse River Modeling and Monitoring Study (ModMon); Phase 1, 1997–1999 Report*, pp. 172, Water Resources Research Institute, Raleigh, NC.

Markus, M., H. Vernon Knapp, and G. D. Tasker (2003), Entropy and generalized least square methods in assessment of the regional value of streamgages, *J. Hydrol.*, *283*, 107–121.

Marshall, K. T. and R. M. Oliver (1995), *Decision Making and Forecasting*, McGraw-Hill, New York.

Mishra, A. K. and P. Coulibaly (2009), Developments in hydrometric network design: A review, *Rev. Geophys.*, *47*, RG2001.

Murphy, B. B. and R. D. Morrison (Eds.) (2002), *Introduction to Environmental Forensics*, Academic Press, San Diego.

National Research Council (2001), Assessing the TMDL Approach to Water Quality Management Report, Washington, D.C.

NC Department of Environment and Natural Resources (1999), Total Maximum Daily Load for Total Nitrogen to the Neuse River Estuary, North Carolina Report, Raleigh, NC.

Ott, W. R. (1995), *Environmental Statistics and Data Analysis*, CRC Press L.L.C, Boca Raton.

Ozkul, S., N. B. Harmancioglu, and V. P. Singh (2000), Entropy-based assessment of water quality monitoring networks, *J. Hydrologic Eng.*, *5*, 90–100.

Paerl, H. W. (1987), Dynamics of Blue-Green Algal (Microcystis Aeruginosa) Blooms in the Lower Neuse River, North Carolina: Causative Factors and Potential Controls Report, Raleigh, N.C.

Paerl, H. W. (2006), Assessing and managing nutrient-enhanced eutrophication in estuarine and coastal waters: Interactive effects of human and climatic perturbations, *Ecol. Eng.*, *26*, 40–54.

Paerl, H. W., M. A. Mallin, C. A. Donahue, M. Go, and B. L. Peierls (1995), Nitrogen loading sources and eutrophication of the Neuse River estuary, North Carolina: Direct and indirect roles of atmospheric deposition Report PB–96–115217/XAB, pp. 130, North Carolina Water Resources Research Inst., Raleigh, NC.

Paerl, H. W., L. M. Valdes, M. F. Piehler, and C. A. Stow (2006), Assessing the effects of nutrient management in an estuary experiencing climatic change: The Neuse River Estuary, North Carolina, *Environ. Manage.*, *37*, 422–436.

Paerl, H. W., L. M. Valdes-Weaver, A. R. Joyner, and V. Winkelmann (2007), Phytoplankton indicators of ecological change in the eutrophying Pamlico Sound system, North Carolina, *Ecol. Appl.*, *17*, 88-101.

Paerl, H. W., K. Rossignol, S. Hall, B. Peierls, and M. Wetz (2009), Phytoplankton community indicators of short- and long-term ecological change in the anthropogenically and climatically impacted Neuse River Estuary, North Carolina, USA, *Estuaries Coasts*, *33*, 485–497.

Paerl, H. W., K. Rossignol, S. Hall, B. Peierls, and M. Wetz (2010), Phytoplankton community indicators of short- and long-term ecological change in the anthropogenically and climatically impacted Neuse River Estuary, North Carolina, USA, *Estuaries Coasts*, *33*, 485–497.

Pinckney, J. L., H. W. Paerl, M. B. Harrington, and K. E. Howe (1998), Annual cycles of phytoplankton community structure and bloom dynamics in the Neuse River Estuary, NC, *Marine Biol.*, *131*, 371–381.

Pollice, A. and G. Jona Lasinio (2010), A multivariate approach to the analysis of air quality in a high environmental risk area, *Environmetrics*, *21*, 741–754.

Puangthongthub, S., S. Wangwongwatana, R. M. Kamens, and M. L. Serre (2007), Modeling the space/time distribution of particulate matter in Thailand and optimizing its monitoring network, *Atmos. Environ.*, *41*, 7788–7805.

Qian, S. S. (1997), Estimating the area affected by phosphorus runoff in an Everglades wetland: A comparison of universal kriging and Bayesian kriging, *Environ. Ecol. Stat.*, *4*, 1–29.

Qian, S. S. and K. H. Reckhow (2007), Combining model results and monitoring data for water quality assessment, *Environ. Sci. Technol.*, *41*, 5008–5013.

Qian, S. S., M. E. Borsuk, and C. A. Stow (2000), Seasonal and long-term nutrient trend decomposition along a spatial gradient in the Neuse River Watershed, *Environ. Sci. Technol.*, *34*, 4474–4482.

Reckhow, K. H. (1996), Improved estimation of ecological effects using an empirical Bayes method, *J. Am. Water Resour. Assoc.*, *32*, 929–935.

Saaty, R. W. (1987), The analytic hierarchy process-what it is and how it is used, *Math. Model.*, *9*, 161–176.

Saaty, T. L. (1977), A scaling method for priorities in hierarchical structures, *J. Math. Psychol.*, *15*, 234–281.

Saaty, T. L. (1986), Axiomatic foundation of the analytic hierarchy process, *Manag. Sci.*, *32*, 841–855.

Saaty, T. L. (1990), *The Analytic Hierarchy Process: Planning, priority setting, resource allocation*, 2nd ed., McGraw-Hill, Pittsburgh, PA.

Saaty, T. L. (1994), *Fundamentals of Decision Making*, RWS Publications, Pittsburgh.

Saaty, T. L. (2005), Analytic Hierarchy Process, in *Encyclopedia of Biostatistics*, Wiley, Chichester, West Sussex.

Sampson, P. D. and P. Guttorp (1992), Nonparametric estimation of nonstationary spatial covariance structure, *J. Am. Stat. Assoc.*, *87*, 108–119.

Sanders, T. G., R. C. Ward, J. C. Loftis, T. D. Steele, D. D. Adrian, and V. Yevjevich (1987), *Design of Networks For Monitoring Water Quality*, 2nd ed., Water Resources Publications, LLC.

Simeonov, V., J. A. Stratis, C. Samara, G. Zachariadis, D. Voutsa, A. Anthemidis, M. Sofoniou, and T. Kouimtzis (2003), Assessment of the surface water quality in Northern Greece, *Water Res.*, *37*, 4119–4124.

Solow, A. R., and A. Gaines, G. (1995), An empirical bayes approach to monitoring water quality, *Environmetrics*, *6*, 1–5.

Stein, W. E. and P. J. Mizzi (2007), The harmonic consistency index for the analytic hierarchy process, *Eur. J. Oper. Res.*, *177*, 488–497.

Stow, C. A., C. Roessler, M. E. Borsuk, J. D. Bowen, and K. H. Reckhow (2003), Comparison of estuarine water quality models for total maximum daily load development in Neuse River Estuary, *J. Water Resour. Plann. Manag.*, *129*, 307–314.

Strobl, R. O. and P. D. Robillard (2008), Network design for water quality monitoring of surface freshwaters: A review, *J. Environ. Manag.*, *87*, 639–648.

Vaidya, O. S. and S. Kumar (2006), Analytic hierarchy process: An overview of applications, *Eur. J. Oper. Res.*, *169*, 1–29.

Valdes-Weaver, L. M., M. F. Piehler, J. L. Pinckney, K. E. Howe, K. Rossignol, and H. W. Paerl (2006), Long-term temporal and spatial trends in phytoplankton biomass and class-level taxonomic composition in the hydrologically variable Neuse-Pamlico Estuarine Continuum, North Carolina, U.S.A, *Limnol. Oceanogr.*, *51*, 1410–1420.

Van Den Honert, R. C. and F. A. Lootsma (1997), Group preference aggregation in the multiplicative AHP The model of the group decision process and Pareto optimality, *Eur. J. Oper. Res.*, *96*, 363–370.

Van Dongen, S. (2006), Prior specification in Bayesian statistics: Three cautionary tales, *J. Theor. Biol.*, *242*, 90–100.

Wahba, G. and J. Wendelberger (1980), Some new mathematical methods for variational objective analysis using splines and cross-validation, *Month. Weather Rev.*, *108*, 1122–1143.

Wilde, F. D. (2005), Preparations for water sampling, in *National field manual for the collection of water-quality data: U.S. Geological Survey Techniques of Water-Resources Investigations*, pp. *46*, U.S. Geological Survey.

Yoon, K. P. and C. L. Hwang (1995), *Multiple attribute decision making: an introduction*, Sage Publications, Thousand Oaks, CA.